NGL-15-003-002 Pub. of the Astronomical Society of the Pacific

Scanner Observations of Selected Cool Stars*

Theodore D. Fay, Jr.

Department of Physics and Astronomy, University of Alabama

William L. Stein and Wayne H. Warren, Jr.

Department of Astronomy, Indiana University

Scanner Observations of Cool Stars

Send Proofs to: William L. Stein
Wayne H. Warren, Jr.
Swain Hall West 319
Department of Astronomy
Indiana University
Bloomington, Indiana 47401

Theodore D. Fay, Jr.
Box 1921
Department of Physics and Astronomy
University of Alabama
University, Alabama 35486

Received: 27 March 1974

*Publications of the Goethe Link Observatory, Indiana University, No. ________

(NASA-CR-138777) SCANNER OBSERVATIONS OF SELECTED COOL STARS (Indiana Univ.) 35 p HC $4.75 CSCL 03A

N74-27348

Unclas

G3/30 41915

ABSTRACT

Photoelectric spectral scans at 30-Å resolution of 9 dwarfs, 10 giants and 6 supergiants with spectral types G0 to M5 are presented. All stars were observed every 4 Å from λ3300 to λ7000. Absorption features observed at this resolution coincide with strong atomic lines of Fe I,II, Ca I,II, MgI, and Na I; vibrational bands of the electronic transitions of TiO, MgH, CaH, SiH, AlH, CN, CH, C_2, OH, and NH. The dependence of the λ3740 Fe I blend and the λ3440 depression on temperature is discussed.

Key Words: spectrophotometry - cool stars - spectral line identification

INTRODUCTION

Much of our information on the nature of cool stars depends upon a comparison of observed fluxes with those from model atmospheres. Previous spectrophotometry in the region 3300-7000 Å has been confined to studies of particular strong atomic and molecular features plus continuum points to determine temperature, gravity and abundance indicators (cf. van den Bergh and Sackman 1965; McClure and van den Bergh 1968; Spinrad and Taylor 1969). There are, however, no published continuous energy distributions of these stars from 3300 to 7000 Å available for detailed comparison with atmospheric models. The scanner observations presented here should be useful for this purpose since the relative fluxes are observed every 4 Å. It is also possible to use these scans to determine line blanketing, identify molecular features, or place narrow-band interference filters for measuring strong absorption features and continuum points in the energy distributions of similar stars.

Figures 1-6 display our scans of G0-M5 stars of different luminosities in the aforementioned wavelength range. Although the resolution is only about 30 Å, we oversample the data at 4-Å intervals both to allow more detailed comparison with models and to increase the accuracy of data reduction. Our resolution is sufficient to show strong atomic lines, molecular bands, and other continuum features. These scans should therefore indicate major sources of line opacity to be included in atmospheric models in this wavelength region.

OBSERVATIONS

The observations were made during 1971 and 1972 at Goethe Link Observatory using equipment previously described by Honeycutt (1971). They were reduced to flux using a method described by Fay, Honeycutt and Warren (1973) and a detailed discussion of observational errors can be found there.

Table I lists the observed energy distributions of the program stars at Hayes (1970) standard wavelengths. All stars have been observed on more than one night, some on as many as five nights. The results presented are means which have been computed by weighting according to nightly errors. For known variables we present only the best individual observations and the corresponding dates are listed in the table. The solar scan shown for comparison in Figure 1 has a resolution of 20 Å and is taken from Labs and Neckel (1968). In order to show the approximate extent of nightly variations for the bright stars, we display in Figures 3 and 6 two scans of μ Cephei taken on different nights.

DISCUSSION

A. Strengths and Identifications of Atomic Line Features

We consider it worthwhile to identify the spectral features found at scanner resolution and to tabulate the strengths of these features. Identification codes for the spectral features in Figures 1-6 are given in Tables II and III. Electronic transitions of molecular bands are indicated by small Greek symbols and strong atomic lines by small Roman symbols.

Many of the atomic line identifications in Table II are Fe I lines of solar equivalent width greater than 1 Å (Moore et al. 1966). Each spectral feature at 30-Å resolution is composed of from 2-10 blended lines. Our atomic line codes are given in column 2 of the first part of Table II while the wavelengths of the lines contributing to each blend are listed in column 3. Solar equivalent widths and lower excitation potentials are given in columns 4 and 5 and are taken from Moore et al. (1966). Column 6 lists the solar identifications of the atomic line blends; there are 43 line blends of H, Fe I, Mg I, Ca I, Ca II, Mn I and Na I included in the table.

In Table IV we tabulate the strengths of some of the line blends identified in Tables II and III. Column 2 lists the wavelengths of the blends and continuum points; the remaining columns tabulate the strengths of line blends in each of the program stars in flux differences measured in magnitudes. An example of the temperature dependence of the Fe I strengths from Table IV is shown in Figure 7. The peak strength of this blend (1f, λ3740) occurs at spectral type K5. The decrease in strength of the λ3740 feature for spectral types later than K5 must be due to some source of opacity which absorbs more at the reference wavelength (λ3680) than at λ3740. Line blanketing by OH and CH is a possible source for this absorption.

Tarafdar and Vardya (1972) show that line blanketing by CH and OH is the strongest opacity source between 3000-4000 Å at temperatures cooler than 5000 K. Vardya (1966) and Greene (1972) have computed partial pressures for OH and CH. For solar abundances, Greene's results show that the partial pressure of OH increases by a factor greater than 1000 as θ varies from 1.0 to 2.2 while the partial pressure of CH decreases by more than 10^6. The computations of Tarafdar and Vardya demonstrate that OH line blanketing decreases sharply between 3500-3800 Å. Therefore we would expect that OH should absorb more at the reference wavelength than at λ3740.

B. Identifications of Molecular Bands

Table III lists the identifications of molecular line blends seen on our scans. The second part of the table defines the molecular codes used in the first part and in the figures. Each electronic transition is given a different Greek letter and/or Arabic number. The first part of the table lists the title of each electronic transition in column 1, the molecular identification code assigned in column 2 and the vibrational band and wavelength of the blend in columns 3 and 4.

Pearse and Gaydon (1963) was used as a general reference for the wavelengths of each molecule considered in Table III. We used the following references to identify the strong TiO features: Gatterer, Junkes, Salpeter and Rosen (1957), Phillips (1969, 1971), Phillips and Davis (1971), Wentink and Spindler (1972). The MgH depressions (Moore et al. 1966) are very strong on our spectra, as can be seen in Figures 1-6. Spinrad and Taylor (1969) have made scanner studies of the strengths of these and the TiO bands in this spectral region. Webber (1971) has identified and studied CaH lines at high resolution in sunspot spectra from λ6200-λ6400. Vardya (1966) indicates that ratios of partial pressures of MgH/CaH are equal to 20 at $\tau = 2/3$ for M4 V. Spinrad and Taylor (1969) have made the most recent scanner studies of the stellar CaH depression at λ6350. As seen in Figures 3-6, our observations are consistent with earlier work.

Sauval (1969) has identified the SiH (0,0) band at λ4140 in sunspot spectra. In the spectrum of β Peg, Davis (1947) finds that next to TiO and MgH, SiH produces the strongest molecular absorption. On our stellar scans in Figures 1-3, these and other SiH bands have been identified. As expected these depressions are weak, since Vardya (1966) gives the partial pressure ratio of MgH/SiH = 30 at $\tau = 2/3$ for M2 V.

Sotirovski (1972) claims to have identified AlH lines from 5000-7000 Å on high resolution sunspot spectra. However Wöhl (1971) has questioned these identifications. According to Davis (1947), the (0,0) transition of AlH at λ4241 is one of the strongest molecular absorption features in β Peg while other transitions are far less conspicuous. Computations by Vardya (1966) indicate that the ratio of partial pressures of MgH to AlH in M2 V stars is about 10 at $\tau = 2/3$. As predicted, features coincident with AlH are at least a factor of three weaker than the MgH features on Figures 1 and 4.

The identifications of the 4γ features have been suggested by Pesch (1972) as due to CaOH. These features are strong only in Barnard's star (BD + 4° 3561, M5 V). Triatomic molecular formation would be likely only at the highest pressures and/or lowest temperatures found in stellar atmospheres.

We now briefly review the known molecular compounds of H, C, N and O which are strong in stellar spectra: CH, OH, NH, CN and C_2. Table III indicates the wavelengths of the stronger bands of these light molecules, and some of their strengths measured from our scans are given in Table IV.

Lambert and Beer (1972) have observed strong OH absorption features in α Orionis near 3 microns. These vibration-rotation bands of OH have f values which are a factor of 100 smaller than the electronic system. Tarafdar and Vardya (1972) have determined that OH is an important opacity source for cool stars in the wavelength range 3000-4000 Å. The bands of the $\Delta v = -1$ sequence of the OH molecule degrade longward of λ3400. The minimum flux in the λ3400 depression seems to occur on our scans near λ3440 for dwarfs.

We have chosen λ3540 as a reference wavelength to measure the λ3440 depression because the highest flux levels between 3300-3600 Å occur at λ3540. A referee has pointed out that the λ3540 reference wavelength is contaminated by the $\Delta v = +1$ sequence of CN beginning at λ3590. Because of this CN contamination, we have confined our analysis to the dwarf stars. For this luminosity class, the λ3590 band is weakest and the dependence of CN absorption upon temperature is minimal as shown by Wing (1967). The range of OH depression strengths shown in Figure 8 exceeds the range in CN strengths given by Wing for the dwarfs. The OH strength is defined by the [0.344] - [0.354]-μ color which is expressed by $-2.5 \log [F_\nu(3440)/F_\nu(3540)]$. The solid line is the relative partial pressure ratio, P_{OH}/P_g, for $\tau = 2/3$ as calculated by Vardya (1966). This OH feature is probably blended with atomic lines given in Table II if the [0.344] - [0.354]-μ color is less than 0.2 magnitudes.

C. Notes on Individual Stars

Binaries

The system ζ Aur is a well known eclipsing binary (see e.g. Wilson 1960). We observed this variable on January 1, 1972 during total eclipse so that only the spectrum of the K4 Ib star is visible. The K4 primary's spectral energy distribution appears normal for its spectral and luminosity class as can be seen from the scans shown in Figures 3 and 6. The α Her AB system is a visual pair. For this system we made an attempt to exclude the secondary from the entrance slot of the scanner by offsetting α Her A from the center of the slot. Since the secondary is a single line spectroscopic binary of type G0 II-III (Deutsch 1960), some contamination of the spectrum is probable shortward of 4000 Å, but the value at each wavelength is difficult to estimate.

The α Sco AB visual system has a separation of only 3" and no attempt was made to exclude the B4 V companion from the entrance slot. Spectral classification of the B4 companion was made by Stone and Struve (1954); the visual magnitude difference of primary and secondary ($\Delta m_{vis} = 4.25$) is from Wierzbinski (1969). If we compare the observed energy distribution of α Ori shown in Figure 3 to the energy distributions of the B stars studied by Faÿ et al. (1973) with the same scanner, we note that an M and B star which differ by 4.2 mag at 5500 Å would differ by less than 0.5 mag at 3800 Å. The weakening of the spectral line features in α Sco at wavelengths shortward of 4000 Å is consistent with the observed visual magnitude differences and derived energy distributions for normal M2 I and B4 V stars.

SUMMARY

Line blanketing features observed at 30-Å resolution for normal stars of spectral classes G0 to M5 can be identified with known atomic or molecular line blends observed in sunspot and stellar spectra of higher resolution. We conclude that many of the atomic line strengths (especially for types later than middle K) are strongly affected at scanner resolution by molecular line blanketing from the electronic transitions of TiO, MgH, CN, CH, OH, C_2, NH, CaH, AlH, and SiH. Observed strengths of the λ3440-OH feature vary approximately with spectral class as do the partial OH pressures computed by Vardya (1966).

ACKNOWLEDGEMENTS

This work was supported by NASA Grant 15-003-002 to Hollis R. Johnson. The authors acknowledge helpful comments and encouragement from R. Kent Honeycutt, R. F. Wing and G. W. Lockwood. We also wish to thank an anonymous referee for his thoroughness and constructive criticism.

FIGURE CAPTIONS

Figure 1. Scans of G, K and M dwarfs in the range λλ3300-5300. Resolution is about 30 Å and data spacing is 4 Å. Identification codes are listed in Tables II and III.

Figure 2. Same as Figure 1 for G, K and M giants.

Figure 3. Same as Figure 1 for G, K and M supergiants.

Figure 4. Scans of G, K and M dwarfs in the range λλ5000-7000. Other comments same as Figure 1.

Figure 5. Same as Figure 4 for G, K and M giants.

Figure 6. Same as Figure 4 for G, K and M supergiants.

Figure 7. Strength of the Fe I depression (in mag) against spectral type. Filled circles are dwarfs, open circles giants, and open triangles supergiants.

Figure 8. Dependence of the OH band depression (λ3440) on temperature for dwarf stars only. The solid line represents calculations by Vardya.

REFERENCES

Bergh, S. van dan, and Sackmann. I. J. 1965, A.J. 70, 353.

Davis, D. N. 1947, Ap.J. 106, 28.

Deutsch, A. J. 1960, in Stellar Atmospheres, J. Greenstein, ed. (Chicago: University of Chicago Press), p. 543.

Fay, T., Honeycutt, R. K. and Warren, W. H. Jr. 1973, A.J. 78, 246.

Getterer, A., Junkes, J., Salpeter, E. W. and Rosen, B. 1957, Molecular Spectra of Metallic Oxides (Vatican City: Vatican Observatory).

Greene, A. E. 1972, Contr. Perkins Obs. Ser. 11, No. 31.

Hayes, D. S. 1970, Ap.J. 159, 165.

Honeycutt, R. K. 1971, Applied Optics 10, 1125.

Labs, D. and Neckel, H. 1968, Zs. f. Ap. 69, 1.

Lambert, D. L. and Beer, R. 1972, Ap.J. 177, 541.

McClure, R. D. and Bergh, S. van den 1968, A.J. 73, 313.

Moore, C. E., Minnaert, M. G. J. and Houtgast, J. 1966, National Bureau of Standards Monograph 61.

Pearse, R. W. B. and Gaydon, A. G. 1963, The Identification of Molecular Spectra (New York: John Wiley and Sons).

Pesch, P. 1972, Ap.J. (Letters) 174, L155.

Phillips, J. G. 1969, Ap.J. 157, 449.

_____________. 1971, Ap.J. 169, 185.

Phillips, J. G. and Davis, S. P. 1971, Ap.J. 167, 209.

Sauval, A. J. 1969, Solar Physics 10, 319.

Sotirovski, P. 1972, Astr. and Ap. Suppl. 6, 85.

Spinrad, H. and Taylor, B. J. 1969, Ap.J. 157, 1279.

Stone, S. N. and Struve, O. 1954 Pub.A.S.P. 66, 191.

Tarafdar, S. P. and Vardya, M. S. 1972, Ap.J. 171, 185.

Vardya, M. S. 1966, M.N.R.A.S. 134, 347.

Webber, J. C. 1971 Solar Physics 16, 340.

Wentink, T. Jr. and Spindler, R. J. Jr. 1972, Journ. Quant. Spectrosc. Radiat. Transfer 12, 1569.

Wierzbinski, S. 1969, Contr. Wroclaw Astr. Obs. No. 16.

Wilson, O. C. 1960, in Stellar Atmospheres, J. Greenstein, ed. (Chicago: University of Chicago Press), p. 436.

Wing, R. F. 1967, Doctoral Dissertation, University of California, Berkeley.

Wöhl, H. 1971, Solar Physics 16, 362.

TABLE I

Relative Magnitudes at Hayes Points Normalized at 5263 Å

Stars*	3400Å	3450Å	3500Å	3571Å	3636Å	3705Å	3862Å	4037Å	4168Å
β Com	$1^{m}.506$	$1^{m}.568$	$1^{m}.440$	$1^{m}.410$	$1^{m}.258$	$1^{m}.150$	$1^{m}.078$	$0^{m}.431$	$0^{m}.433$
τ Cet			1.695	1.775	1.476	1.429	1.547	0.777	0.642
ε Eri			2.000	2.270	1.715	1.810	2.110	1.020	0.843
61 Cyg A			2.811	3.027	2.754	2.621	2.857	1.660	1.337
61 Cyg B			3.114	3.212	2.966	2.851	2.983	1.931	1.511
GRM 1618					2.895	2.821	2.657	1.879	1.539
LA 21185								1.815	1.621
+15° 2620								1.870	1.626
+4° 3561									
31 Com	1.797	1.779	1.710	1.681	1.599	1.336	1.225	0.665	0.563
ε Vir	2.174	2.205	2.090	2.306	1.792	1.665	2.268	0.950	1.043
α UMa	2.647	2.758	2.579	2.785	2.255	2.119	2.421	1.187	1.238
α Boo	3.171	3.206	3.004	3.258	2.691	2.568	2.931	1.506	1.445
α Hya			3.915	3.990	3.523	3.429	3.779	2.152	2.065
α Tau			3.730	3.938	3.502	3.451	3.594	2.238	1.968
α Cet			4.071	4.266	3.796	3.587	3.571	2.379	2.081
δ Vir			4.151	4.129	3.709	3.610	3.480	2.303	1.905
ω Vir			3.982	4.036	3.515	3.461	3.317	2.163	1.717
α Her A (6/23/71)					3.195	3.068	2.926	1.759	1.402
ε Gem			3.574	3.670	2.923	2.882	3.243	1.880	1.938
ζ Aur (1/1/72)				4.080	3.552	3.390	3.615	2.320	2.165
σ CMa							3.598	2.385	2.181
α Sco AB				4.088	3.898	3.753	3.495	2.608	2.317
α Ori (2/5/72)					3.996	3.903	3.648	2.594	2.245
μ Cep (10/31/71)							4.056	3.373	2.809

*Date indicated if star is variable.

TABLE I (continued)

4255Å	4464Å	4566Å	4787Å	5000Å	5263Å	5559Å	5841Å	6057Å	6439Å	6793Å
$0^{m}.422$	$0^{m}.243$	$0^{m}.165$	$0^{m}.066$	$0^{m}.047$	$0^{m}.000$	$-0^{m}.149$	$-0^{m}.187$	$-0^{m}.220$	$-0^{m}.260$	$-0^{m}.308$
0.676	0.334	0.229	0.107	0.065	0.000	-0.170	-0.243	-0.292	-0.378	-0.453
0.829	0.357	0.155	0.034	0.079	0.000	-0.203	-0.369	-0.427	-0.527	-0.669
1.433	0.685	0.364	0.340	0.215	0.000	-0.190	-0.279	-0.338	-0.463	-0.553
1.595	0.781	0.425	0.461	0.296	0.000	-0.495	-0.741	-0.817	-0.985	-1.055
1.602	0.781	0.422	0.461	0.345	0.000	-0.514	-0.728	-0.794	-1.038	-1.074
1.796	0.894	0.579	0.482	0.479	0.000	-0.337	-0.523	-0.604	-0.884	-0.711
1.855	0.820	0.620	0.561	0.429	0.000	-0.605	-1.005	-1.175	-1.621	-1.590
2.993	1.718	1.198	1.402	0.715	0.000	-0.083	-0.651	-0.700	-1.314	-1.148
0.518	0.344	0.254	0.102	0.070	0.000	-0.194	-0.263	-0.300	-0.341	-0.398
0.782	0.450	0.336	0.126	0.103	0.000	-0.232	-0.368	-0.425	-0.530	-0.651
0.920	0.552	0.386	0.137	0.080	0.000	-0.304	-0.451	-0.518	-0.595	-0.691
1.229	0.707	0.493	0.241	0.169	0.000	-0.363	-0.562	-0.676	-0.788	-0.929
1.690	0.945	0.658	0.290	0.133	0.000	-0.448	-0.675	-0.818	-0.954	-1.130
1.716	0.945	0.611	0.431	0.272	0.000	-0.474	-0.717	-0.882	-1.082	-1.193
1.895	1.095	0.735	0.540	0.349	0.000	-0.497	-0.769	-0.985	-1.282	-1.358
1.789	1.048	0.700	0.671	0.528	0.000	-0.362	-0.487	-0.739	-1.141	-1.057
1.670	1.170	0.823	0.898	0.770	0.000	-0.259	-0.349	-0.678	-1.239	-1.138
1.419	1.296	0.858	0.984	0.889	0.000	-0.443	-0.638	-0.968	-1.564	-1.552
1.411	0.938	0.673	0.191	0.146	0.000	-0.429	-0.622	-0.703	-0.727	-0.865
1.804	1.065	0.747	0.366	0.178	0.000	-0.600	-0.885	-1.052	-1.219	-1.453
1.787	1.150	0.715	0.318	0.181	0.000	-0.524	-0.755	-0.974	-1.210	-1.402
2.074	1.471	1.059	0.611	0.396	0.000	-0.543	-0.813	-1.023	-1.388	-1.534
2.008	1.394	0.952	0.556	0.376	0.000	-0.589	-0.843	-1.127	-1.443	-1.524
2.602	1.960	1.457	0.902	0.554	0.000	-0.581	-0.970	-1.267	-1.624	-1.802

TABLE II

Atomic Line Blends at 30 Å Resolution

Blend No.	Atomic Code	Wave-length Å	Solar Weq Å	Low EP eV	Solar Ident.
1	7a	3361.2	0.9	0.9	TiI,TiII
2	6a	3380.9	0.8	0.4	Ni I
		3384.0	0.4	3.0	Fe I
		3394.0	0.6	0.0	Ni I
3	6b	3414.8	0.8	0.0	Ni I
		3433.6	0.5	0.0	Ni I
		3446.2	0.5	0.1	Ni I
	1a	3440.6	1.2	0.0	Fe I
4	6c	3458.5	0.7	0.2	Ni I
		3461.7	0.8	0.0	Ni I
		3465.9	0.5	0.1	Fe I
5	1b	3475.4	0.6	0.1	Fe I
		3476.7	0.5	0.1	Fe I
		3490.6	0.8	0.0	Fe I
		3497.8	0.7	0.1	Fe I
	6d	3493.0	0.8	0.1	Ni I
6	6e	3510.3	0.5	0.2	Ni I
		3515.1	0.7	0.1	Ni I
		3524.5	1.3	0.0	Ni I
7	1c	3565.4	1.0	1.0	Fe I
		3570.1	1.4	0.9	Fe I
		3581.2	2.1	0.9	Fe I
		3585.3	0.8	1.0	Fe I
		3587.0	0.5	1.0	Fe I
8	1d	3608.9	1.0	1.0	Fe I
		3618.8	1.4	1.0	Fe I
		3631.5	1.4	1.0	Fe I
		3647.9	1.0	0.9	Fe I
9	1e	3679.6	0.5	0.0	Fe I
		3687.5	0.6	0.0	Fe I
		3705.6	0.6	0.0	Fe I
10	2e	3646.0			Balmer Limit
11	1f	3721.9	0.5	10.2	H 14
	or	3719.9	1.6	0.0	Fe I
	2f	3722.6	0.7	0.0	TiI + FeI
		3727.6	0.6	1.0	Fe I
		3734.4	1.0	10.2	H 13
		3734.9	3.0	0.9	Fe I
		3737.1	1.1	0.0	Fe I
		3743.4	0.6	1.0	Fe I
		3745.6	1.2	0.1	Fe I
		3749.5	1.9	0.9	Fe I
		3750.1	1.4	10.2	H 12
		3758.2	1.6	1.0	Fe I
		3763.8	0.8	1.0	Fe I
		3767.2	0.8	1.0	Fe I
		3770.6	1.9	10.2	H 11
12	1g	3797.9	3.5	10.2	H 10
	or	3795.0	0.5	1.0	Fe I
	2g	3799.6	0.6	1.0	Fe I
		3815.9	1.3	1.5	Fe I
		3820.4	1.7	0.9	Fe I
		3825.9	1.5	0.9	Fe I
		3824.4	0.5	0.0	Fe I
		3827.8	0.9	1.6	Fe I
		3834.2	0.6	1.0	Fe I
	3a	3829.3	0.9	2.7	Mg I
		3832.0	1.7	2.7	Mg I
		3838.3	1.9	2.7	Mg I
		3835.4	2.4	10.2	H 9
		3840.4	0.6	1.0	Fe I
13	1h	3856.4	0.7	0.0	Fe I
	or	3859.9	1.6	0.0	Fe I
	2h	3872.5	0.6	1.0	Fe I
		3878.0	0.6	1.0	Fe I
		3878.6	0.7	0.0	Fe I
		3886.3	0.9	0.0	Fe I
		3889.0	2.3	10.2	H 8
14	8a	3905.5	0.9	1.9	Si I
15	4a	3933.7	20	0.0	Ca II K
	4b	3968.5	15	0.0	Ca II H
16	1i	4045.8	1.2	1.5	Fe I
		4063.6	0.8	1.6	Fe I
		4071.7	0.7	1.6	Fe I
17	2d	4101.7	3.1	10.2	H δ
18	1j	4132.0	0.4	1.6	Fe I
		4143.9	0.5	1.6	Fe I
19	5a	4226.7	1.5	0.0	Ca I
20	G	4250.8	0.4	1.6	Fe I
		4260.5	0.6	2.4	Fe I
		4271.8	0.8	1.5	Fe I
		4254.3	0.4	0.0	Cr I
		4271.1	0.2	3.1	Cr I
		4274.8	0.2	0.0	Cr I
		4283.0	0.1	1.9	Ca I
		4302.5	0.2	1.9	Ca I
		4307.9	0.7	1.6	Fe I
		4325.8	0.8	1.6	Fe I
21	2c	4340.5	2.9	10.2	H γ
22	1k	4383.6	1.0	1.5	Fe I
		4404.8	0.9	1.6	Fe I
		4415.0	0.4	1.6	Fe I

TABLE II (continued)

Blend No.	Atomic Code	Wave-length Å	Solar Weq Å	Low EP eV	Solar Ident.
23	5b	4423.3	0.1	2.1	Na I
		4425.4	0.1	1.9	Ca I
		4427.3	0.1	0.0	Fe I
		4435.0	0.2	1.9	Ca I
		4435.7	0.1	1.9	Ca I
		4444.5	0.4	2.0	Fe I
		4454.8	0.2	1.9	Ca I
24	1ℓ	4522.5	0.1	2.8	Fe II
		4525.1	0.1	3.6	Fe I
		4526.4	0.1	3.9	Fe 1
		4528.6	0.3	2.2	Fe I
		4529.5	0.1	1.6	Ti II
		4531.2	0.1	1.5	Fe I
		4534.0	0.1	1.2	Ti II
		4549.5	0.2	2.0	FeII+TiII
25	5c	4581.4	0.2	2.5	CaI + FeI
		4585.9	0.1	2.5	Ca I
		4578.6	0.1	2.5	Ca I
		4583.9	0.1	3.1	FeI + Fe II
26	1m	4637.5	0.1	3.2	Fe I
		4654.6	0.2	2.0	Fe I
		4668.1	0.1	3.4	Fe I
27	3a	4703.0	0.3	4.3	Mg I
		4707.3	0.1	3.2	Fe I
		4709.0	0.1	2.0	Ti I
		4710.3	0.1	3.0	Fe I
		4714.4	0.1	3.4	Ni I
		4727.4	0.1	3.6	Fe + Mn
		4736.8	0.1	3.2	Fe
28	9a	4754.0	0.1	2.0	Mn I
		4762.4	0.1	2.9	Mn I
		4768.4	0.1	3.7	Fe I
		4783.4	0.2	2.3	Mn I
		4786.5	0.1	3.4	Ni I
29	2b	4861.3	3.7	10.2	H β
	1n	4871.3	0.2	2.9	Fe I
		4872.1	0.2	2.9	Fe I
		4878.2	0.2	2.9	CaI + Fe I
		4890.8	0.2	2.9	Fe I
		4891.5	0.3	2.9	Fe I
30	1o	4919.0	0.3	2.9	Fe I
		4920.5	0.5	2.9	Fe I
		4923.9	0.2	2.9	Fe II
		4924.8	0.1	2.2	Fe I
31	1p	4957.6	0.7	2.8	Fe I

Blend No.	Atomic Code	Wave-length Å	Solar Weq Å	Low EP eV	Solar Ident.
32	1q	4978.6	0.1	4.0	Fe I
		4980.2	0.1	3.6	Ni I
		4981.7	0.1	0.9	Ti I
		4982.5	0.1	4.1	Fe I
		4983.2	0.1	4.2	Fe I
		4983.8	0.1	4.1	Fe I
		4985.2	0.1	3.9	Fe I
		4985.5	0.1	2.9	Fe I
		4991.0	0.1	0.8	Ti I
		4994.1	0.1	0.9	Fe I
		4999.5	0.1	0.8	Ti I
		5001.9	0.2	3.9	Fe I
		5005.7	0.1	3.9	Fe I
		5006.1	0.2	2.8	Fe I
		5007.3	0.2	0.8	Ti I
		5012.0	0.2	0.8	Fe I
		5014.2	0.2	0.0	Ti I
		5015.0	0.1	3.9	Fe I
		5018.4	0.2	2.9	Fe II
33	1r	5035.4	0.1	3.6	Ni I
		5035.9	0.1	1.5	Ti I
		5040.9	0.1	4.3	Fe I
		5041.0	0.1	1.0	Fe I
		5041.8	0.2	1.5	Fe I
		5049.8	0.1	2.2	Fe I
		5051.6	0.1	0.9	Fe I
		5065.0	0.1	4.3	Fe I
		5068.8	0.1	2.9	Fe I
		5074.7	0.1	4.2	Fe I
34	3b	5167.3	1.0	2.7	MgI + FeI
		5172.7	1.3	2.7	Mg I
		5183.6	1.6	2.7	Mg I
35	1s	5188.7	0.2	1.6	TiII+CaI
		5191.5	0.2	3.0	Fe I
		5192.4	0.2	3.0	Fe I
		5193.0	0.1	0.0	Ti I
		5194.9	0.2	1.6	Fe I
		5202.3	0.2	2.2	Fe I
		5204.5	0.2	0.9	CrI+FeI
		5206.0	0.2	0.9	Cr I
		5208.4	0.2	0.9	Cr I
36	1t	5227.2	0.3	1.6	Fe I
	or	5233.0	0.3	2.9	Fe I
	5d	5264.0	0.2	2.5	Ca I
		5265.6	0.1	2.5	Ca I
		5266.5	0.3	0.8	Ti I
		5269.5	0.5	0.9	Fe I
		5270.3	0.3	1.6	CaI + FeI
		5273.2	0.1	3.3	Fe I
		5273.4	0.1	2.5	Fe I
		5276.1	0.1	2.9	Cr I
		5281.7	0.2	3.0	Fe I
		5283.6	0.2	3.2	Fe I

TABLE II (continued)

Blend No.	Atomic Code	Wave-length Å	Solar Weq Å	Low EP eV	Solar Ident.
37	1u	5324.0	0.3	3.2	Fe I
		5328.0	0.4	0.9	Fe I
		5328.5	0.2	1.6	Fe I
		5332.9	0.1	1.6	Fe I
		5339.9	0.2	3.2	Fe I
		5341.1	0.2	1.6	Fe I
38	1v	5371.5	0.3	1.0	Fe I
		5384.4	0.2	4.3	Fe I
		5393.2	0.2	3.2	Fe I
		5397.1	0.2	0.9	Fe I
		5400.5	0.1	4.4	Fe I
		5404.1	0.2	4.3	Fe I
		5405.8	0.3	1.0	Fe I
		5415.2	0.2	4.4	Fe I
		5424.0	0.2	4.3	Fe I
		5429.8	0.3	1.0	Fe I
		5434.5	0.2	1.0	Fe I
		5446.9	0.2	1.0	Fe I
		5455.6	0.2	1.0	Fe I
39	5e	5582.0	0.1	2.5	Ca I
		5588.8	0.1	2.5	Ca I
		5590.1	0.1	2.5	Ca I
		5594.5	0.1	2.5	Ca I
		5598.4	0.1	2.5	Ca I
		5601.3	0.1	2.5	Ca I
		5602.9	0.1	2.5	Ca I
		5615.6	0.3	2.5	Ca I
40	D	5890.0	0.8	0.0	Na I
		5896.0	0.6	0.0	Na I
41	5f	6102.7	0.1	1.9	Ca I
		6122.2	0.2	1.9	Ca I
		6136.6	0.1	2.4	Fe I
		6137.7	0.1	2.6	Fe I
		6141.7	0.1	3.6	Fe I
		6162.2	0.2	1.9	Ca I
		6169.5	0.1	2.5	Ca I
42	5g	6439.0	0.2	2.5	Ca I
		6462.6	0.2	2.5	CaI + FeI
43	2a	6562.8	4.0	10.2	H α

Atomic Line Code Identification

Code	Atom
1	Fe I
2	H(Balmer)
3	Mg I
4	Ca II
5	Ca I
6	Ni I
7	Ti I
8	Si I
9	Mn I

TABLE III

MOLECULAR BANDS AT 30-Å RESOLUTION

ELECTRONIC SYSTEM	MOLECULAR CODE	VIBRATION BAND	WAVELENGTH Å
$C^3\Delta$-$X^3\Delta$ (TiO)	$1\alpha_3$	3,0	4584
		4,1	4626
		5,2	4668
	$1\alpha_2$	2,0	4761
		3,1	4804
		4,2	4848
	$1\alpha_1$	1,0	4954
		2,1	4999
	$1\alpha_0$	0,0	5167
		?	5307
		?	5356
	$1\alpha_{-1}$	0,1	5448
		1,2	5497
	$1\alpha_{-2}$	0,2	5760
		1,3	5810
$a^1\Delta$-$C^1\Phi$ (TiO)	$1\beta_0$	0,0	5600
		1,1	5631
		2,2	5663
		3,3	5697
		4,4	5727
$A^3\Phi$-$X^3\Delta$ (TiO)	$1\gamma_2$	2,0 R_2	6322
		3,1 R_3	6358
		4,2 R_2	6448
		5,3 R_1	6512
	$1\gamma_1$	1,0 R_3	6651
		1,0 R_2	6680
		1,0 R_1	6713
		2,1 R_2	6746
		3,2 R_2	6814
		4,3 R_2	6852
	$1\gamma_0$	0,0 R_3	7053
		0,0 R_2	7087
		0,0 R_1	7124
		1,1 R_1	7197
		2,2 R_3	7270
$B^3\Pi$-$X^3\Delta$ (TiO)	$1\gamma'_1$	1,0 R_1	5847
		2,1 R_3	5951
		3,2 R_3	6003
		4,3 R_3	6058
	$1\gamma'_0$	0,0 R_1	6158
		0,0 R_2	6186
		0,0 R_3	6214
		1,1 R_2	6240
		1,1 R_2	6276
	$1\gamma'_{-1}$	0,1 R_1	6569
		0,1 R_2	6596
		0,1 R_3	6629
		1,2 R_2	6649
$e^1\Sigma$-$d^1\Sigma$ (TiO)	$1\epsilon_0$	0,0	4114

TABLE III (continued)

ELECTRONIC SYSTEM	MOLECULAR CODE	VIBRATION BAND	WAVELENGTH Å
$D^3\Pi - X^3\Delta$ (TiO)	1η	0,0	3286-3650
$A^2\Pi - X^2\Sigma$ (MgH)	$2\alpha_1$	1,0	4845
	$2\alpha_0$	0,0 R	5211
		0,0 Q	5186
		1,1	5182
		2,2	5155
	$2\alpha_{-1}$	0,1	5621
		1,2	5559
		2,3	5516
	$2\alpha_{-2}$	0,2	6083
$A^2\Pi - X^2\Sigma$ (CaH)	$2\beta_0$	0,0 Q_2	6920
		0,0 P_2	7035
$B^2\Sigma - X^2\Sigma$ (CaH)	$2\beta_{-1}$	0,1	7567
	$2\gamma_0$	0,0	6346
$A^1\Pi - X^1\Sigma$ (AlH)	$3\alpha_1$	1,0	4066
	$3\alpha_0$	0,0	4241
		1,1	4357
		2,2	4450
	$3\alpha_{-1}$	0,1 R	4546
		0,1Q	4576

ELECTRONIC SYSTEM	MOLECULAR CODE	VIBRATION BAND	WAVELENGTH Å
	$3\alpha_{-2}$	0,2 R	4886
		0,2 Q	4929
		1,3	5031
	$3\alpha_{-3}$	0,3	5314
		1,4	5430
$C^1\Sigma - A^1\Pi$ (AlH)	$3\beta_0$	0,0	4723
$E^1\Pi - A^1\Pi$ (AlH)	$3\gamma_0$	0,0	3382
$b^3\Pi - a^3\Pi$ (AlH)	$3\delta_0$	0,0	3810
$A^2\Delta - X^2\Delta$ (SiH)	$3\epsilon_1$	1,0	3870
	$3\epsilon_0$	0,0 Q_1	4128
		0,0 Q_2	4142
		1,1	4190
		2,2	4270
(CaOH)	4γ		5550
			5730
			6038
			6230
			6415
$A^2\Delta - X^2\Pi$ (CH)	$5\alpha_0$	0,0	4320
	$5\alpha_{-1}$	0,1	4890

TABLE III (continued)

ELECTRONIC SYSTEM	MOLECULAR CODE	VIBRATION BAND	WAVELENGTH Å
$B^2\Sigma - X^2\Pi$ (CH)	$5\beta_0$	0,0	3880
		1,1	4030
	$5\beta_{-1}$	1,2	4496
$A^2\Pi - X^2\Sigma$ (CN)	$6\alpha_7$	8,1	4832
		9,2	4936
		10,3	5043
	$6\alpha_6$	6,0	5129
		7,1	5239
		8,2	5354
		9,3	5473
		10,4	5598
	$6\alpha_5$	5,0	5606
		6,1	5730
		7,2	5858
		8,3	5993
		9,4	6132
	$6\alpha_4$	4,0	6192
		5,1	6332
		6,2	6478
		7,3	6631
		8,4	6791
$B^2\Sigma - X^2\Sigma$ (CN)	$6\beta_1$	1,0	3590
	$6\beta_0$	0,0	3883
	$6\beta_{-1}$	0,1	4216
	$6\beta_{-2}$	0,2	4606
		1,3	4578

ELECTRONIC SYSTEM	MOLECULAR CODE	VIBRATION BAND	WAVELENGTH Å
$A^3\Pi g - X'^3\Pi u$ (C_2 SWAN)	7α	0,0	5165
		0,1	5635
	$8\alpha_0$	1,1 Q	3370
		0,0 Q	3360
		0,0 R	3302
	$8\alpha_{-1}$	0,1 P	3676
		0,1 Q	3638
	$8\alpha_{-2}$	0,2	4320
$A^2\Sigma^+ - X^2\Pi$ (OH)	$9\alpha_{-1}$	0,1 R	3430
		0,1 Q	3465
	$9\alpha_{-2}$	0,2 R	3890
		0,2 Q	3933
	$9\alpha_{-3}$	0,3 R	4450
		0,3 Q	4506

TABLE III (continued)

MOLECULAR CODE IDENTIFICATION

CODE	MOLECULE	CODE	MOLECULE
1α-η	TiO	5α,β	CH
2α	MgH	6α,β	CN
2β,γ	CaH	7α	C_2 SWAN
3α-δ	AlH	8α	NH
3ε	SiH	9α	OH
4γ	CaOH		

TABLE IV

LINE BLEND DEPRESSIONS IN MAGNITUDES

Figure Code	Color MICRONS	Stars (G and K Dwarfs)						
		β Com G0V	Sun* G2V	τ Cet G8V	ε Eri K2V	61 Cyg K5V	61 Cyg B K7V	Groom. 1618 M0V
$6\alpha + 8\alpha_0$	[0.336] - [0.340]	0.13	0.15	0.35	0.50	0.34	0.30	---
$6b,d + 9\alpha_{-1} + 1a,b$	[0.344] - [0.354]	0.20	0.28	0.36	0.50	0.50	0.60	0.7?
$1c,d + 6\beta_1$	[0.358] - [0.368]	0.30	0.40	0.38	0.50	0.72	0.50	0.4
$1f + 2f$	[0.374] - [0.368]	0.14	0.29	0.29	0.57	0.70	0.50	0.4
$4a,b + 9\alpha_{-2}$	[0.393] - [0.402]	0.70	1.00	0.75	0.85	1.05	0.80	0.79
$5a + 6\beta_{-1}$	[0.423] - [0.426]	0.01	0.1	0.01	0.03	0.10	0.28	0.25
G	[0.430] - [0.436]	0.22	0.40	0.29	0.43	0.50	0.50	0.54
$1k + 3\alpha_0$	[0.439] - [0.436]	0.00	0.20	0.03	0.08	0.08	0.05	0.10
$1\alpha_2 + 2\alpha_1$	[0.479] - [0.472]	-0.03	0.10	-0.03	-0.07	0.10	0.08	0.17
$2\alpha_0 + 3b$	[0.518] - [0.524]	0.09	0.18	0.19	0.30	0.46	0.49	0.50
$D + 1\alpha_{-2}$	[0.589] - [0.582]	0.06	0.06	0.06	0.08	0.28	0.33	0.45
$6\alpha_5 + 4\beta_0 + 1\gamma_1'$	[0.602] - [0.608]	0.02	0.00	0.02	0.03	0.05	0.05	0.02
$1\gamma_0'$	[0.618] - [0.613]	-0.01	0.00	-0.02	-0.02	-0.02	0.03	0.03
$2\gamma_0$	[0.638] - [0.634]	-0.01	0.00	-0.02	0.00	-0.01	0.01	0.03

*Solar scans by Labs and Neckel are at 20-Å resolution and narrow features show deeper depressions than our scans.

TABLE IV (continued)

Stars (M dwarfs and giants)

Figure Code	Color MICRONS	La 21185 M2V	15° 2620 M2V	4° 3561 M5V	α Cet M1.5III	δ Vir M3III	ω Vir M5III	α Her A M5Ib-II
$6a + 8\alpha_0$	[0.336] - [0.340]	---	---	---	0.2?	0.06	-0.1	-0.1
$6b,d + 9\alpha_{-1} + 1a,b$	[0.344] - [0.354]	1.1	---	---	0.40	0.51	0.55	0.45
$1c,d + 6\beta_1$	[0.356] - [0.366]	0.3	---	---	0.68	0.69	0.7	0.8
1f + 2f	[0.374] - [0.368]	0.3	---	---	0.40	0.37	0.27	0.25
$4a,b + 9\alpha_{-2}$	[0.393] - [0.402]	0.77	1.0	---	1.29	1.25	1.15	1.34
$5a + 6\beta_{-1}$	[0.423] - [0.426]	0.5	0.3	---	0.25	0.31	0.30	0.35
G	[0.430] - [0.436]	0.27	0.33	---	0.54	0.43	0.35	0.32
$1k + 3\alpha_0$	[0.439] - [0.436]	0.0	0.01	---	0.07	0.06	0.00	0.03
$1\alpha_2 + 2\alpha_1$	[0.479] - [0.472]	0.16	0.25	0.2	0.05	0.15	0.28	0.22
$1\alpha_1$	[0.497] - [0.494]	0.16	0.19	0.25	0.16	0.37	0.66	1.05
$2\alpha_0 + 3b$	[0.518] - [0.524]	0.45	0.54	0.65	0.31	0.46	0.46	0.49
$D + 1\alpha_{-2}$	[0.589] - [0.582]	0.57	0.57	0.95	0.26	0.43	0.53	0.56
$6\alpha_2 + 4\beta_0 + 1\gamma_1'$	[0.602] - [0.608]	0.1	0.13	0.22	0.14	0.21	0.25	0.25
$1\gamma_0'$	[0.620] - [0.613]	0.42	0.45	0.90	0.30	0.55	0.70	0.68
$2\gamma_0$	[0.638] - [0.634]	0.08	0.07	0.10	-0.08	-0.12	-0.19	0.15

TABLE IV (continued)

Figure Code	Color MICRONS	Stars (G and K giants) 31 Com G0III	ε Vir G8IIIab	α UMa $K0^{-}$IIIa	α Boo K2IIIp	α Hya K3II-III	α Tau K5III
6a + $8\alpha_0$	[0.336] - [0.340]	0.1	0.15	0.21	0.17	0.1	0.2
6b,d + $9\alpha_{-1}$ + 1a,b	[0.344] - [0.354]	0.2	0.12	0.21	0.30	0.30	0.32
1c,d + $6\beta_1$	[0.358] - [0.368]	0.30	0.68	0.74	0.75	0.80	0.74
1f + 2f	[0.374] - [0.368]	0.17	0.28	0.35	0.44	0.55	0.58
4a,b + $9\alpha_{-2}$	[0.393] - [0.400]	0.69	0.94	0.99	1.28	1.30	1.35
5α + $6\beta_{-1}$	[0.423] - [0.426]	0.02	0.03	0.06	0.07	0.21	0.25
G	[0.430] - [0.436]	0.23	0.32	0.38	0.43	0.52	0.55
1k + $3\alpha_0$	[0.439] - [0.436]	0.03	0.05	0.06	0.05	0.06	0.1
$1\alpha_2$ + $2\alpha_1$	[0.479] - [0.472]	-0.05	-0.1	-0.1	-0.07	-0.1	0.06
$1\alpha_1$	[0.497] - [0.494]	0.00	0.00	0.00	0.00	-0.01	0.06
$2\alpha_0$ + 3b	[0.518] - [0.524]	0.07	0.11	0.14	0.20	0.26	0.30
D + $1\alpha_{-2}$	[0.589] - [0.582]	0.06	0.06	0.1	0.04	0.1	0.21
$6\alpha_5$ + $4\beta_0$ + $1\gamma_1'$	[0.602] - [0.608]	0.02	0.03	0.04	0.03	0.07	0.1
$1\gamma_0'$	[0.618] - [0.613]	-0.01	-0.04	-0.003	0.02	-0.05	0.13
$2\gamma_0$	[0.638] - [0.634]	-0.03	-0.04	-0.03	-0.03	-0.04	0.06

TABLE IV (continued)

Figure Code	Color MICRONS	Stars (supergiants) ϵ Gem G8Ib	ζ Aur A K4Ib	σ CMa K7Ib	α Sco M1.5Iab	α Ori M1-M2Ia-Ib	μ Cep M2Ia
6a + $8\alpha_0$	[0.386] - [0.340]	0.3	0.0	---	---	---	---
6b,d + $9\alpha_{-1}$ + 1a,b	[0.344] - [0.354]	0.1	0.0	---	---	0.1	---
1c,d + $6\beta_1$	[0.358] - [0.368]	0.70	0.85	---	0.43	0.50	---
1f + 2f	[0.374] - [0.368]	0.27	0.45	---	0.05	0.18	---
4a,b + $9\alpha_{-2}$	[0.393] - [0.402]	1.15	1.25	1.27	0.7	1.17	1.3
5a + $6\beta_{-1}$	[0.423] - [0.426]	0.09	0.2	0.29	0.21	0.21	0.3
G	[0.430] - [0.436]	0.41	0.56	0.63	0.49	0.55	0.66
1k + $3\alpha_0$	[0.438] - [0.432]	0.09	0.08	0.09	0.07	0.09	0.07
$1\alpha_2$ + $2\alpha_1$	[0.479] - [0.472]	-0.17	-0.09	-0.05	-0.06	-0.03	-0.07
$1\alpha_1$	[0.497] - [0.494]	-0.02	-0.04	0.07	0.14	0.16	0.19
$2\alpha_0$ + 3b	[0.518] - [0.524]	0.12	0.31	0.31	0.25	0.27	0.31
D + $1a_{-2}$	[0.589] - [0.582]	0.06	0.06	0.27	0.26	0.33	0.33
$6\alpha_5$ + $4\beta_0$ + $1\gamma_1'$	[0.602] - [0.608]	0.04	0.08	0.12	0.16	0.16	0.18
$1\gamma_0'$	[0.618] - [0.613]	0.00	0.02	0.12	0.22	0.28	0.26
$2\gamma_0$	[0.638] - [0.634]	-0.05	-0.05	-0.12	-0.13	-0.13	-0.10

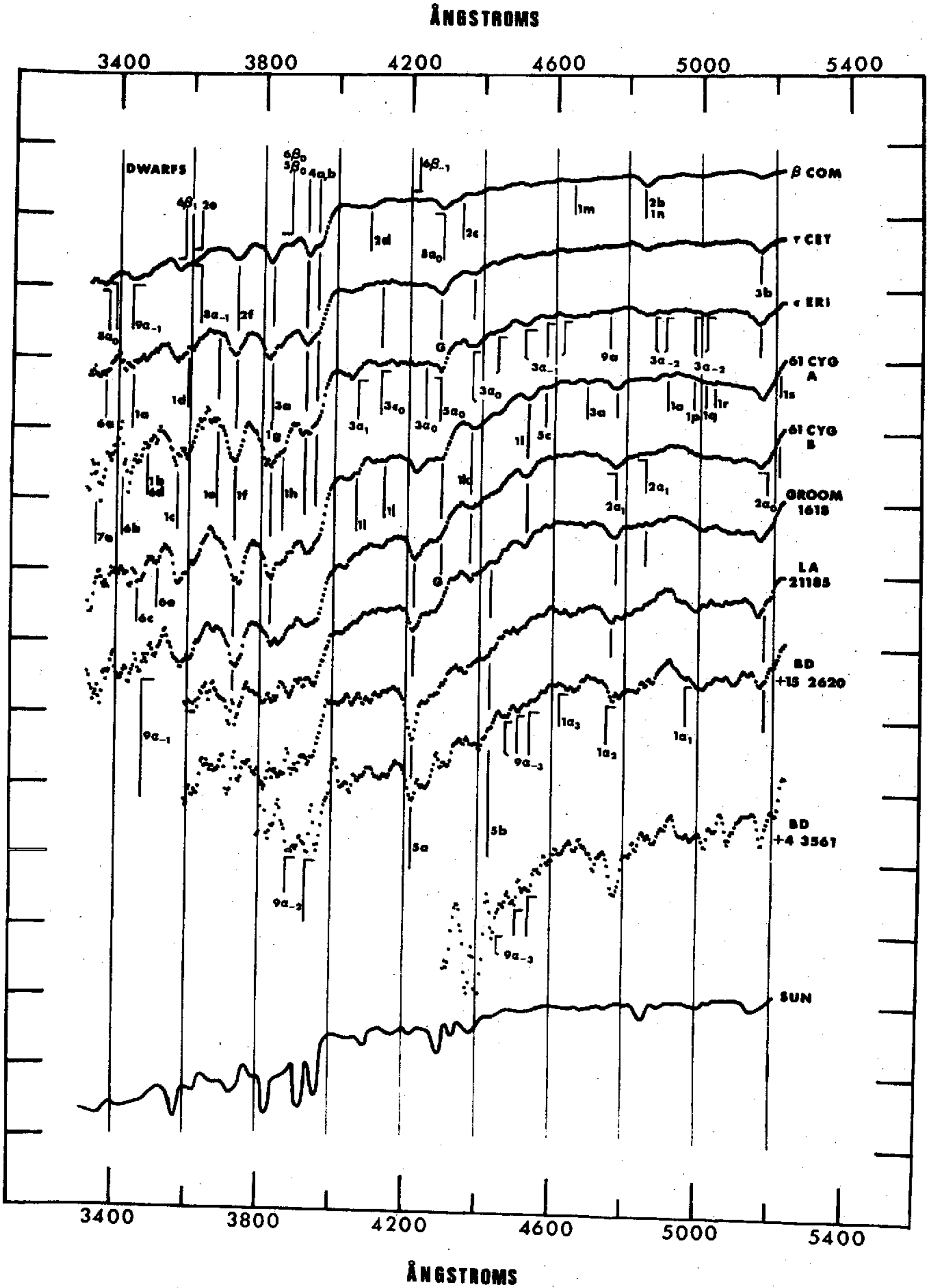
ÅNGSTROMS
3400
3800
4200
4600
5000
5400
DWARFS
β COM
γ CET
ε ERI
61 CYG A
61 CYG B
GROOM 1618
LA 21185
BD +15 2620
BD +4 3561
SUN
ÅNGSTROMS

Fig 1

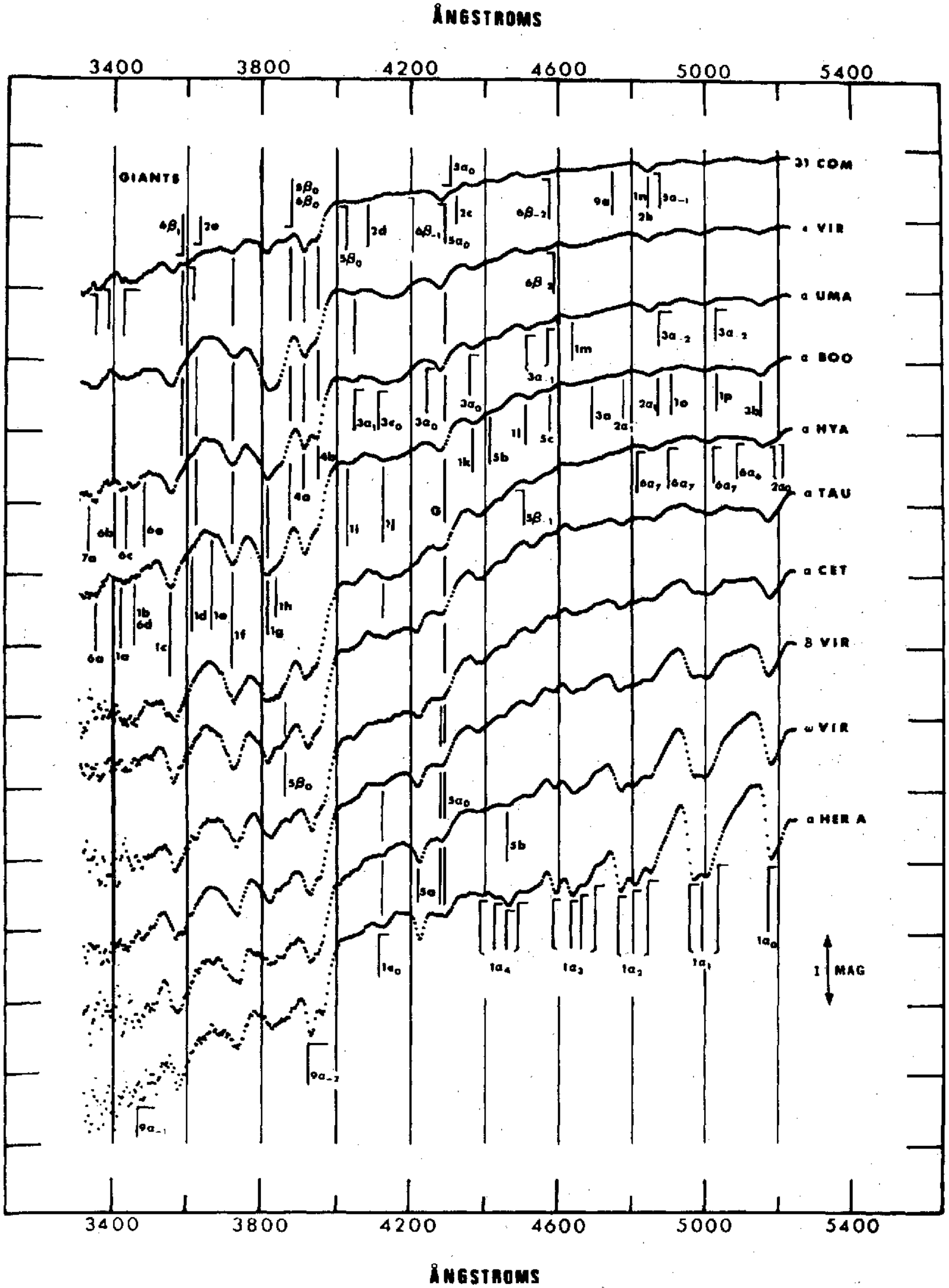
ÅNGSTROMS
3400
3800
4200
4600
5000
5400
GIANTS
31 COM
ε VIR
α UMA
α BOO
α HYA
α TAU
α CET
δ VIR
ω VIR
α HER A
1 MAG
3400
3800
4200
4600
5000
5400
ÅNGSTROMS

Fig 2

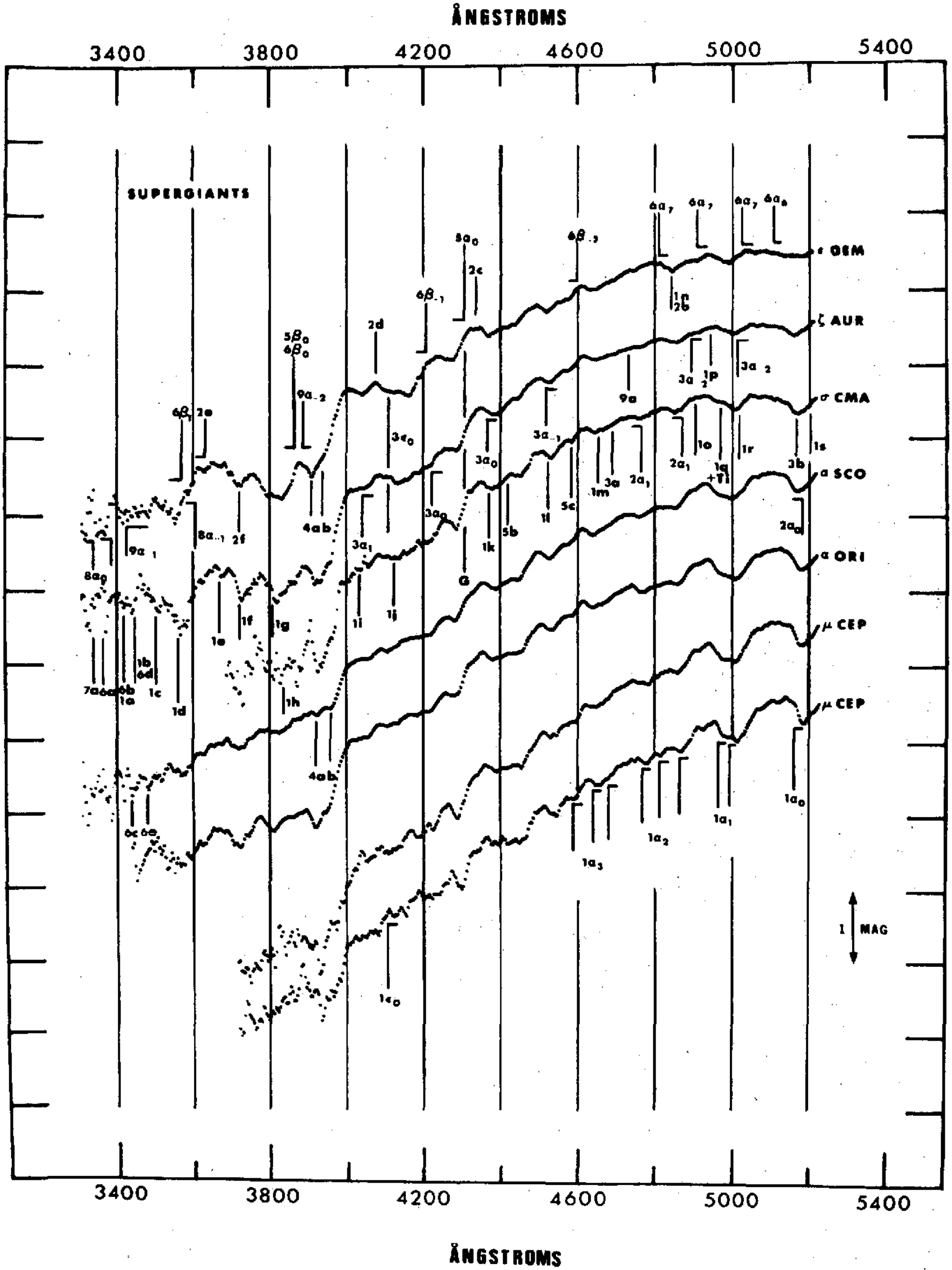
ÅNGSTROMS
3400
3800
4200
4600
5000
5400
SUPERGIANTS
ε GEM
ζ AUR
σ CMA
α SCO
α ORI
μ CEP
μ CEP
1 MAG
3400
3800
4200
4600
5000
5400
ÅNGSTROMS

Fig 3

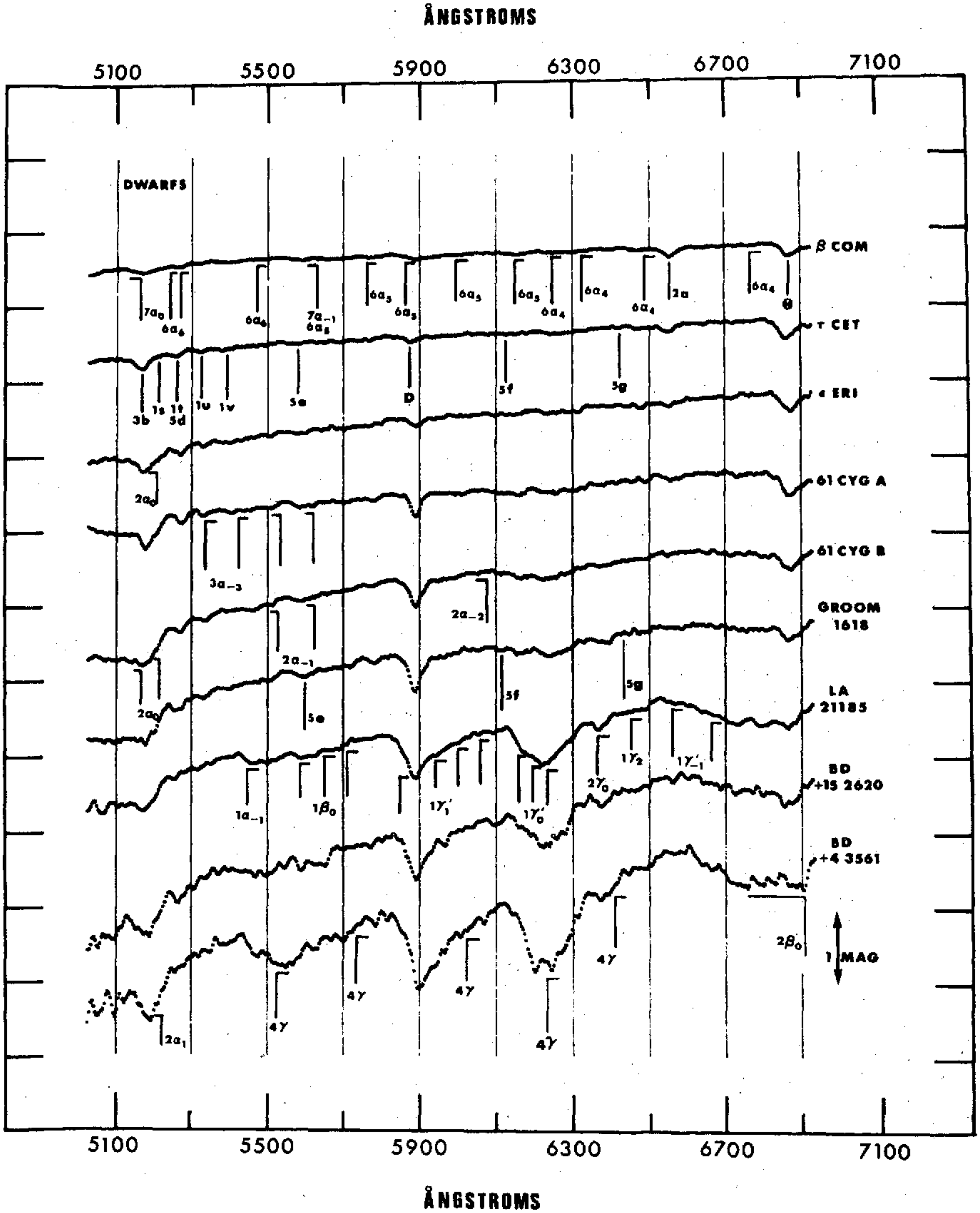
ÅNGSTROMS
5100
5500
5900
6300
6700
7100
DWARFS
β COM
τ CET
ε ERI
61 CYG A
61 CYG B
GROOM 1618
LA 21185
BD +15 2620
BD +4 3561
1 MAG
ÅNGSTROMS

fig 4

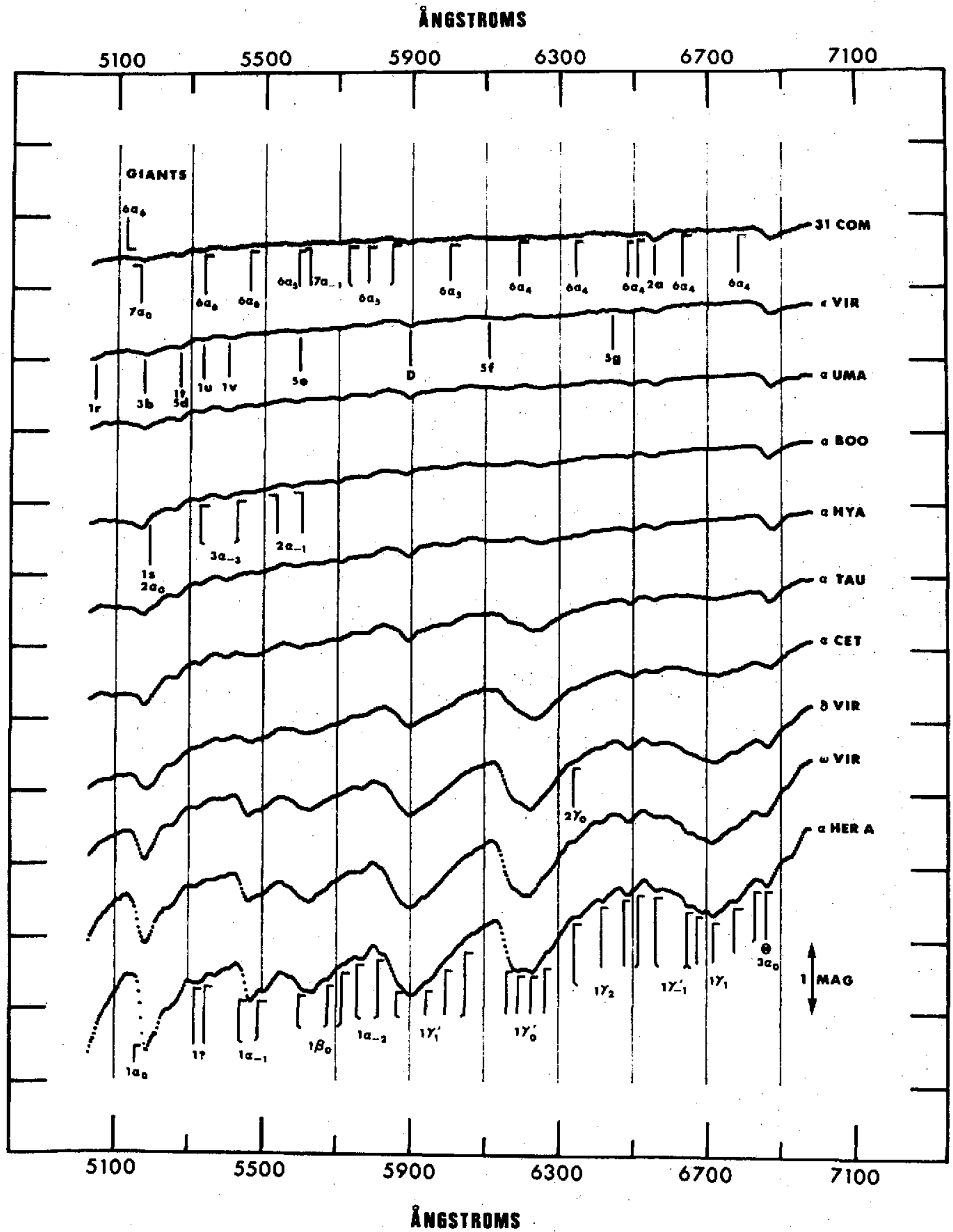
ÅNGSTROMS
5100
5500
5900
6300
6700
7100
GIANTS
31 COM
α VIR
α UMA
α BOO
α HYA
α TAU
α CET
δ VIR
ω VIR
α HER A
1 MAG
D
5e
5f
5g
1u
1v
3b
1r
1s
2a₀
3a₋₃
2a₋₁
7a₀
6a₆
6a₅
6a₄
2a
2γ₀
1γ₂
1γ′₋₁
1γ₁
3a₀
1a₀
1?
1α₋₁
1β₀
1a₋₂
1γ′₁
1γ′₀
ÅNGSTROMS

Fig 5

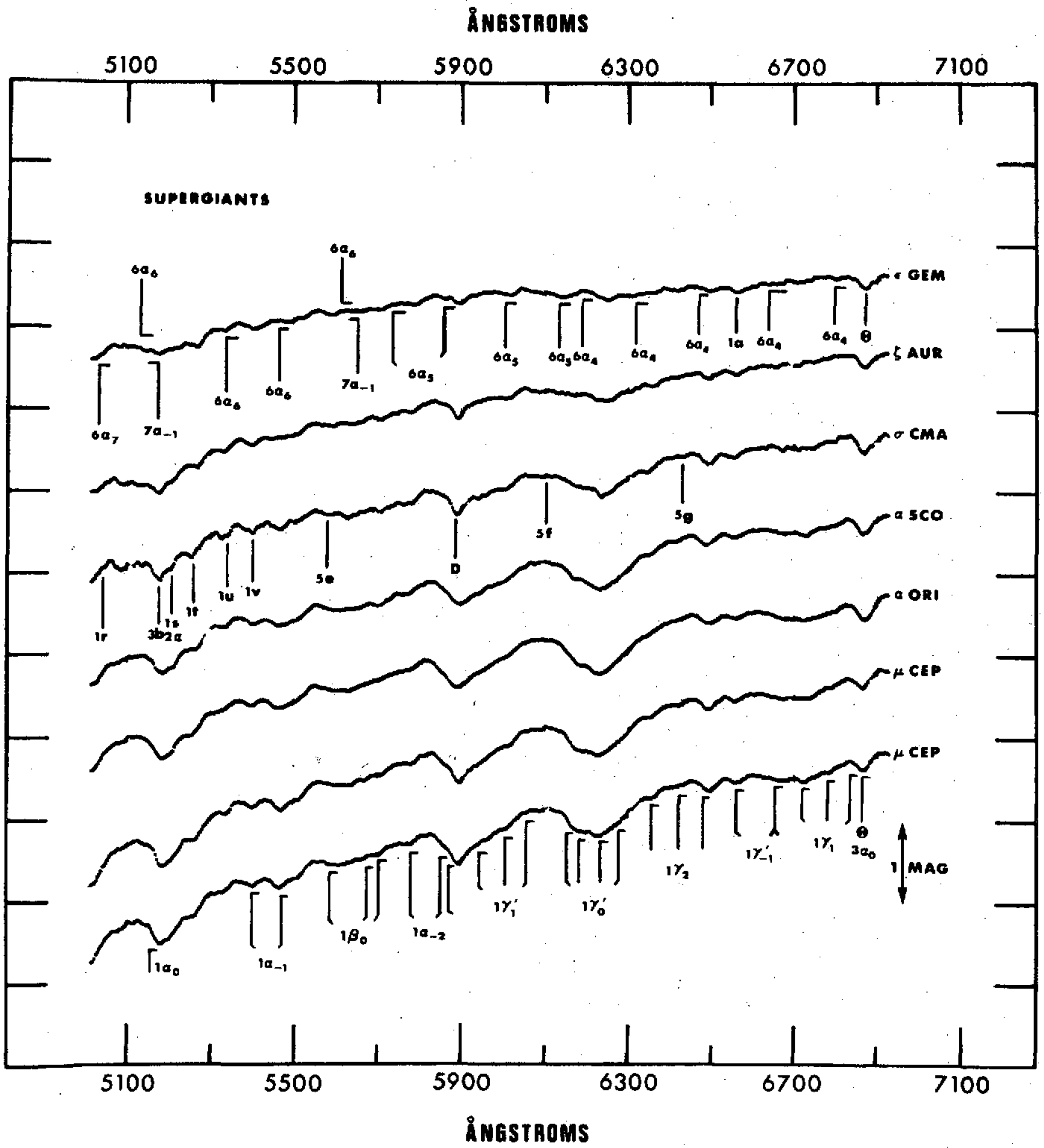
ÅNGSTROMS
5100
5500
5900
6300
6700
7100
SUPERGIANTS
ε GEM
ζ AUR
σ CMA
α SCO
α ORI
μ CEP
μ CEP
1 MAG
ÅNGSTROMS

Fig 1

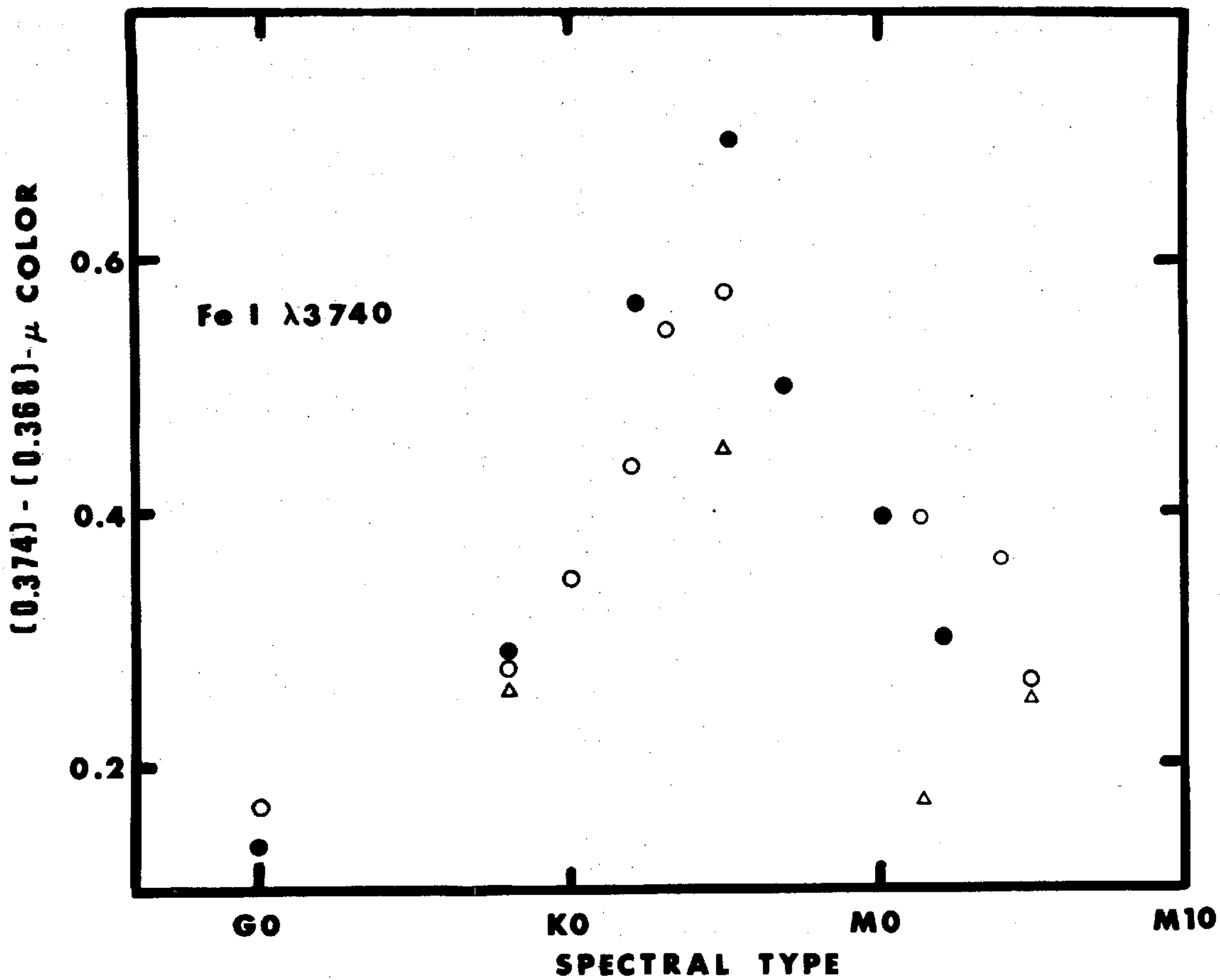

Fig 7

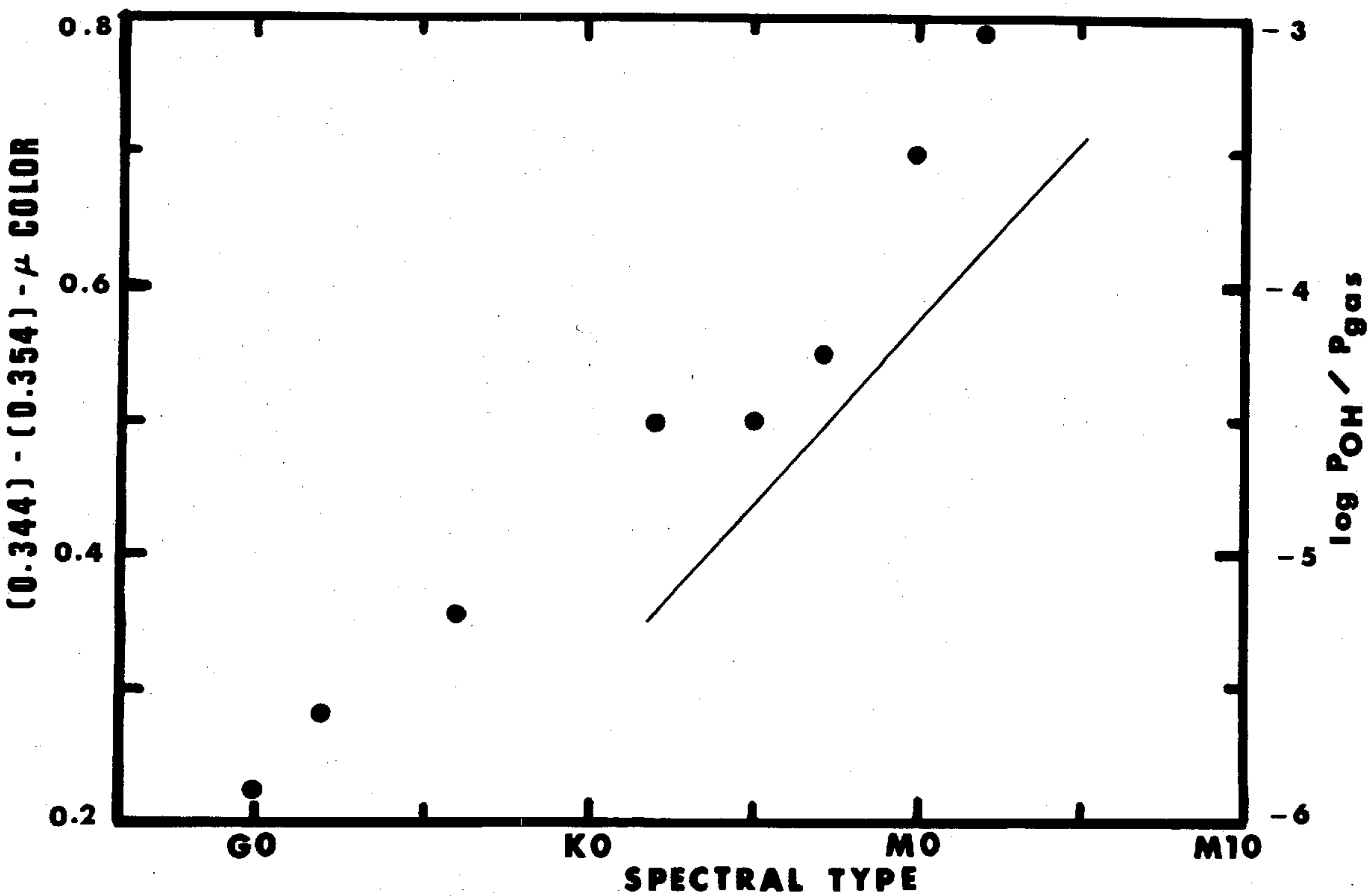
0.8
0.6
0.4
0.2
(0.344) - (0.354) - μ COLOR
G0
K0
M0
M10
SPECTRAL TYPE
-3
-4
-5
-6
log P_{OH} / P_{gas}

Fig 8